



Search for Structure in the $B_s^0\pi^\pm$ Invariant Mass Spectrum

R. Aaij *et al.**

(LHCb Collaboration)

(Received 2 August 2016; published 5 October 2016; corrected 6 March 2017)

The $B_s^0\pi^\pm$ invariant mass distribution is investigated in order to search for possible exotic meson states. The analysis is based on a data sample recorded with the LHCb detector corresponding to 3 fb^{-1} of pp collision data at $\sqrt{s} = 7$ and 8 TeV. No significant excess is found, and upper limits are set on the production rate of the claimed $X(5568)$ state within the LHCb acceptance. Upper limits are also set as a function of the mass and width of a possible exotic meson decaying to the $B_s^0\pi^\pm$ final state. The same limits also apply to a possible exotic meson decaying through the chain $B_s^{*0}\pi^\pm, B_s^{*0} \rightarrow B_s^0\gamma$ where the photon is excluded from the reconstructed decays.

DOI: [10.1103/PhysRevLett.117.152003](https://doi.org/10.1103/PhysRevLett.117.152003)

Interest in exotic hadrons has recently intensified, with a wealth of experimental data becoming available [1,2]. All the well-established exotic states contain a heavy quark-antiquark ($c\bar{c}$ or $b\bar{b}$) pair together with additional light particle content. However, the D0 Collaboration has reported evidence [3] of a narrow structure, referred to as the $X(5568)$, in the $B_s^0\pi^\pm$ spectrum produced in $p\bar{p}$ collisions at center-of-mass energy $\sqrt{s} = 1.96$ TeV. The claimed $X(5568)$ state, if confirmed, would differ from any of the previous observations, as it must have constituent quarks with four different flavors (b, s, u, d). As such, it would be unique among observed exotic hadrons in having its mass dominated by a single constituent quark rather than by a quark-antiquark pair. This could provide a crucial piece of information to help understand how exotic hadrons are bound; specifically, whether they are dominantly tightly bound (often referred to as “tetraquarks” and “pentaquarks”) or loosely bound meson-meson or meson-baryon molecules.

In this Letter, results are presented from a search for an exotic meson, denoted X , decaying to $B_s^0\pi^\pm$ in a data sample corresponding to 3 fb^{-1} of pp collision data at $\sqrt{s} = 7$ and 8 TeV recorded by LHCb. The search is performed by scanning over the mass and width of the purported state, with dedicated fits for parameters corresponding to those of the claimed $X(5568)$ state. The B_s^0 mesons are reconstructed in decays to $D_s^-\pi^+$ and $J/\psi\phi$ final states to obtain a B_s^0 yield approximately 20 times larger than that used by the D0 Collaboration. The inclusion of charge-conjugate processes is implied throughout the Letter. The analysis techniques follow closely those

developed for studies of the B^+K^- [4], $B^+\pi^-$ and $B^0\pi^+$ [5] spectra. As in previous analyses, the charged pion which is combined with the B_s^0 meson in order to form the $B_s^0\pi^\pm$ candidate is referred to as the “companion pion”.

The LHCb detector [6,7] is a single-arm forward spectrometer covering the pseudorapidity range $2 < \eta < 5$, designed for the study of particles containing b or c quarks. The detector includes a high-precision tracking system consisting of a silicon-strip vertex detector surrounding the pp interaction region, a large-area silicon-strip detector located upstream of a dipole magnet with a bending power of about 4 Tm, and three stations of silicon-strip detectors and straw drift tubes placed downstream of the magnet. The tracking system provides a measurement of momentum, p , of charged particles with a relative uncertainty that varies from 0.5% at low momentum to 1.0% at 200 GeV (units in which $c = \hbar = 1$ are used throughout). The minimum distance of a track to a primary vertex (PV), the impact parameter, is measured with a resolution of $(15 + 29/p_T)\text{ }\mu\text{m}$, where p_T is the component of the momentum transverse to the beam, in GeV. Different types of charged hadrons are distinguished using information from two ring-imaging Cherenkov detectors. Photons, electrons, and hadrons are identified by a calorimeter system consisting of scintillating-pad and preshower detectors, an electromagnetic calorimeter, and a hadronic calorimeter. Muons are identified by a system composed of alternating layers of iron and multiwire proportional chambers. The online event selection is performed by a trigger, which consists of a hardware stage, based on information from the calorimeter and muon systems, followed by a software stage, which applies a full event reconstruction.

Simulations of pp collisions are generated using PYTHIA [8] with a specific LHCb configuration [9]. Decays of hadronic particles are described by EVTGEN [10], in which final-state radiation is generated using PHOTOS [11]. The interaction of the generated particles with the detector, and

*Full author list given at the end of the article.

Published by the American Physical Society under the terms of the [Creative Commons Attribution 3.0 License](https://creativecommons.org/licenses/by/3.0/). Further distribution of this work must maintain attribution to the author(s) and the published article's title, journal citation, and DOI.

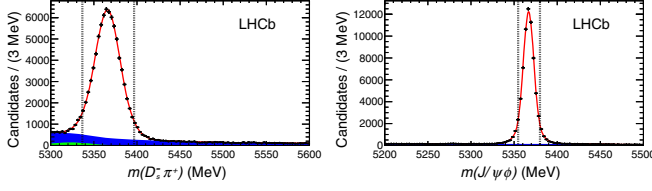


FIG. 1. Selected candidates for (left) $B_s^0 \rightarrow D_s^- \pi^+$ and (right) $B_s^0 \rightarrow J/\psi \phi$ decays, with $p_T(B_s^0) > 5$ GeV, where the B_s^0 signal window requirements of $|m(D_s^- \pi^+) - 5367 \text{ MeV}| < 30 \text{ MeV}$ and $|m(J/\psi \phi) - 5367 \text{ MeV}| < 13 \text{ MeV}$ are indicated by dotted lines. Results of the fits described in the text are superimposed with the total fit result shown as a red line, the signal component as an unfilled area, the combinatorial background component as a dark blue area, and additional background contributions as a light green area.

its response, are implemented using the GEANT4 toolkit [12] as described in Ref. [13].

Candidate B_s^0 mesons are reconstructed through the decays $B_s^0 \rightarrow D_s^- \pi^+$ with $D_s^- \rightarrow K^+ K^- \pi^-$, and $B_s^0 \rightarrow J/\psi \phi$ with $J/\psi \rightarrow \mu^+ \mu^-$ and $\phi \rightarrow K^+ K^-$. Particle identification, track quality, and impact parameter requirements are imposed on all final-state particles. Both B_s^0 and intermediate particle (D_s^- and J/ψ) candidates are required to have good vertex quality and to have invariant mass close to the known values [14]. Specific backgrounds due to other b -hadron decays are removed with appropriate vetoes. A requirement is imposed on the multiplicity of tracks originating from the PV associated with the B_s^0 candidate; this requirement is about 90% efficient on the B_s^0 signal and significantly reduces background due to random $B_s^0 \pi^\pm$ combinations. To further reduce background, the p_T of the B_s^0 candidate, $p_T(B_s^0)$, is required to be greater than 5 GeV. Results are also obtained with this requirement increased to 10 or 15 GeV, to be more sensitive to scenarios in which the X state is predominantly produced from hard

processes. The definition of the fiducial acceptance is completed with the requirements $p_T(B_s^0) < 50$ GeV and $2.0 < y < 4.5$, where y is the rapidity of the B_s^0 candidate.

The signals in the two B_s^0 decay modes are shown in Fig. 1. To estimate the B_s^0 yields, the data are fitted with functions that include a signal component, described by a double Gaussian function with a shared mean, and a combinatorial background component, described by a polynomial function. Backgrounds from $B_s^0 \rightarrow D_s^\mp K^\pm$ decays in the $D_s^- \pi^+$ sample and from $\Lambda_b^0 \rightarrow J/\psi p K^-$ decays in the $J/\psi \phi$ sample, where a final-state hadron is misidentified, are modeled using empirical shapes derived from simulated samples. An additional component, modeled with a Gaussian function, is included to account for possible $B^0 \rightarrow J/\psi K^+ K^-$ decays [15] in the $J/\psi \phi$ sample. The results of these fits are reported in Table I. The signal-to-background ratio in the B_s^0 signal windows is about 10 for the $D_s^- \pi^+$ sample and above 50 for the $J/\psi \phi$ sample.

The B_s^0 candidates are combined with each track originating from the associated PV that gives a good quality $B_s^0 \pi^\pm$ vertex and that has $p_T > 500$ MeV. A loose pion identification requirement is imposed in order to suppress possible backgrounds involving misidentified particles. In case multiple candidates are obtained in the same event, all are retained. Mass and vertex constraints are imposed [16] in the calculation of the $B_s^0 \pi^\pm$ invariant mass.

In order to obtain quantitative results on the contributions from resonant structures in the data, the $B_s^0 \pi^\pm$ mass distributions are fitted with a function containing components for the signal and background. The signal shape is an S -wave Breit–Wigner function multiplied by a function that accounts for the variation of the efficiency with $B_s^0 \pi^\pm$ mass. The efficiency function, determined from simulation, plateaus at high $B_s^0 \pi^\pm$ mass and falls near the threshold to a value that depends on $p_T(B_s^0)$. The resolution is better

TABLE I. Yields, N , of B_s^0 and $X(5568)$ candidates obtained from the fits to the B_s^0 and $B_s^0 \pi^\pm$ candidate mass distributions, with statistical uncertainties only. The values reported for $N(B_s^0)$ are those inside the B_s^0 signal window. The reported values for $X(5568)$ are obtained from fits with signal mass and width parameters fixed to those determined by the D0 Collaboration. Relative efficiencies $\epsilon^{\text{rel}}(X)$ of the B_s^0 and $X(5568)$ candidate selection criteria are also given. The reported uncertainties on the relative efficiencies are only statistical, due to the finite size of the simulated samples.

		$B_s^0 \rightarrow D_s^- \pi^+$	$B_s^0 \rightarrow J/\psi \phi$	Sum
$N(B_s^0)/10^3$	$p_T(B_s^0) > 5$ GeV	62.2 ± 0.3	43.6 ± 0.2	105.8 ± 0.4
	$p_T(B_s^0) > 10$ GeV	28.4 ± 0.2	13.2 ± 0.1	41.6 ± 0.2
	$p_T(B_s^0) > 15$ GeV	8.8 ± 0.1	3.7 ± 0.1	12.5 ± 0.1
$N(X)$	$p_T(B_s^0) > 5$ GeV	3 ± 64	-33 ± 43	-30 ± 77
	$p_T(B_s^0) > 10$ GeV	75 ± 52	12 ± 33	87 ± 62
	$p_T(B_s^0) > 15$ GeV	14 ± 31	-10 ± 17	4 ± 35
$\epsilon^{\text{rel}}(X)$	$p_T(B_s^0) > 5$ GeV	0.127 ± 0.002	0.093 ± 0.001	...
	$p_T(B_s^0) > 10$ GeV	0.213 ± 0.003	0.206 ± 0.002	...
	$p_T(B_s^0) > 15$ GeV	0.289 ± 0.005	0.290 ± 0.004	...

than 1 MeV and does not affect the results. The background is modeled with a polynomial function. It is verified that this function gives a good description of backgrounds composed of either a real or a fake B_s^0 decay combined with a random pion, as determined from simulation or from data in B_s^0 candidate mass sideband regions, respectively.

For each choice of signal mass and width parameters, a binned maximum likelihood fit to the $B_s^0\pi^\pm$ candidate mass spectrum is used to determine the signal and background yields and the parameters of the polynomial shape that describes the background. The two B_s^0 decay modes are fitted simultaneously. The results of the fit where the mass and width are fixed according to the central values obtained by the D0 collaboration, $m = 5567.8 \pm 2.9(\text{stat})_{-1.9}^{+0.9}(\text{syst})$ MeV and $\Gamma = 21.9 \pm 6.4(\text{stat})_{-2.5}^{+5.0}(\text{syst})$ MeV [3], are shown in Fig. 2 for both B_s^0 decay modes combined. The $X(5568)$ yield is not significant for any minimum $p_T(B_s^0)$ requirement. In each case, the change in negative log likelihood between fits including or not including the signal component is less than 2 units for two additional free parameters corresponding to the yields in the two B_s^0 decay modes. The results of the fits are summarized in Table I.

The yields N obtained from the fits are used to measure the ratio of cross sections

$$\rho_X^{\text{LHCb}} \equiv \frac{\sigma(pp \rightarrow X + \text{anything}) \times \mathcal{B}(X \rightarrow B_s^0\pi^\pm)}{\sigma(pp \rightarrow B_s^0 + \text{anything})}, \quad (1)$$

$$= \frac{N(X)}{N(B_s^0)} \times \frac{1}{\epsilon^{\text{rel}}(X)}, \quad (2)$$

where the cross sections σ are for promptly produced particles within the LHCb acceptance. Since $\sigma(pp \rightarrow B_s^0 + \text{anything})$ in the LHCb acceptance has been previously measured [17], any result for ρ_X^{LHCb} can be scaled to give a result for $\sigma(pp \rightarrow X + \text{anything}) \times \mathcal{B}(X \rightarrow B_s^0\pi^\pm)$ in the LHCb acceptance. The relative efficiency $\epsilon^{\text{rel}}(X) = \epsilon(X)/\epsilon(B_s^0)$ accounts for the reconstruction and selection efficiency of the companion pion as well as the requirement that it is within the LHCb acceptance. These effects are determined from simulation, weighted to reproduce the measured differential B_s^0 production spectrum [17], together with a data-driven evaluation [18] of the efficiency of the particle identification requirement on the companion pion. In the simulation, the X state is assumed to be spinless; it has been verified that the systematic uncertainty associated with this choice is negligible. The quantities used to evaluate ρ_X^{LHCb} are summarized in Table I.

Systematic uncertainties are assigned due to possible biases in the evaluation of $N(X)$, $N(B_s^0)$, and $\epsilon^{\text{rel}}(X)$. The signal shape is modified by varying the efficiency function, and separately by changing the assumed angular momentum in the relativistic Breit–Wigner function from S wave to P wave. In each case, the changes in $N(X)$ are assigned

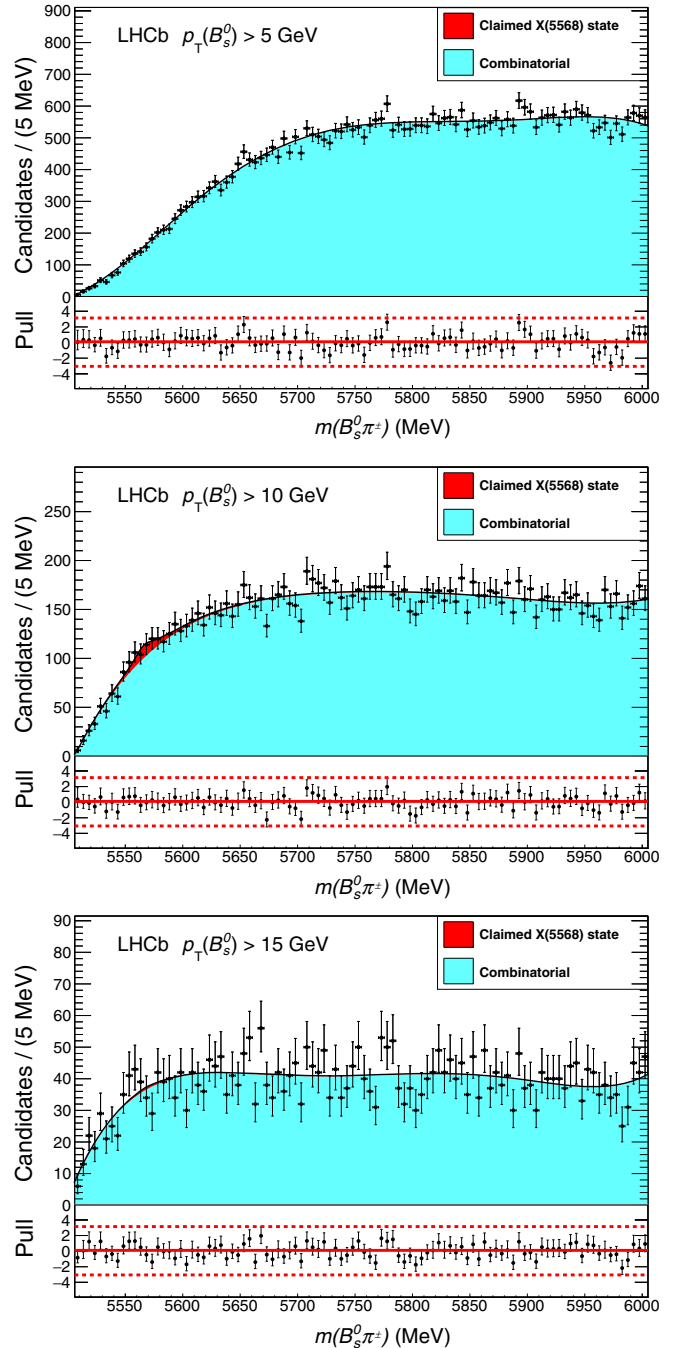


FIG. 2. Results of the fit to the $B_s^0\pi^\pm$ mass distribution for candidates (both B_s^0 modes combined) with minimum $p_T(B_s^0)$ of (top) 5 GeV, (middle) 10 GeV, and (bottom) 15 GeV. The component for the claimed $X(5568)$ state is included in the fit but is not significant. The distributions of the normalized residuals, or “pulls,” displayed underneath the main figures show good agreement between the fit functions and the data.

as the associated systematic uncertainties. Uncertainties associated with the determination of $N(B_s^0)$ arise due to the size of the B_s^0 sample and the estimation of the background in the signal region. In addition to the limited size of the

simulation sample, uncertainties associated with $e^{\text{rel}}(X)$ arise due to the precision with which the companion pion reconstruction and particle identification efficiencies are known [18,19]. The uncertainties from different sources are combined in quadrature and give a total that is much smaller than the statistical uncertainty. To obtain results that can be compared to those for the claimed $X(5568)$ state reported by the D0 Collaboration, additional systematic uncertainties are assigned from the changes in the results for ρ_X^{LHCb} when the mass and width parameters are varied independently within $\pm 1\sigma$ ranges from their central values. These are the dominant sources of systematic uncertainty.

To cross-check the results, candidates are selected with criteria similar to those used in the observation of $B_c^+ \rightarrow B_s^0 \pi^+$ decays [20], with consistent results. In addition, $B^0 \rightarrow D^- \pi^+$ decays are used to create $B^0 \pi^+$ combinations, and the results on the excited B states of Ref. [5] are reproduced.

The values of ρ_X^{LHCb} for the two B_s^0 decay modes are consistent and are therefore combined in a weighted average. In the average, systematic uncertainties are taken to be uncorrelated between the two B_s^0 decay modes. An exception is made when obtaining results corresponding to the claimed $X(5568)$ state, where the uncertainty due to the limited precision of the reported mass and width values [3] is treated as correlated between the two modes. These results are

$$\begin{aligned}\rho_X^{\text{LHCb}}[p_T(B_s^0) > 5 \text{ GeV}] &= -0.003 \pm 0.006 \pm 0.002, \\ \rho_X^{\text{LHCb}}[p_T(B_s^0) > 10 \text{ GeV}] &= 0.010 \pm 0.007 \pm 0.005, \\ \rho_X^{\text{LHCb}}[p_T(B_s^0) > 15 \text{ GeV}] &= 0.000 \pm 0.010 \pm 0.006,\end{aligned}$$

where the first uncertainty is statistical and the second is systematic. Since the signal is not significant, upper limits on ρ_X^{LHCb} are obtained by integration of the likelihood in the positive region to find the value that contains the fraction of the integral corresponding to the required confidence level (C.L.). The upper limits at 90 (95)% C.L. are found to be

$$\begin{aligned}\rho_X^{\text{LHCb}}[p_T(B_s^0) > 5 \text{ GeV}] &< 0.011 (0.012), \\ \rho_X^{\text{LHCb}}[p_T(B_s^0) > 10 \text{ GeV}] &< 0.021 (0.024), \\ \rho_X^{\text{LHCb}}[p_T(B_s^0) > 15 \text{ GeV}] &< 0.018 (0.020).\end{aligned}$$

No significant signal for a $B_s^0 \pi^\pm$ resonance is seen at any value of mass and width in the range considered. To obtain limits on ρ_X^{LHCb} for different values of these parameters, fits are performed for widths (Γ) of 10 to 50 MeV in 10 MeV steps. For each width, the mass is scanned in steps of $\Gamma/2$, starting one unit of width above the kinematic threshold and ending approximately one and a half units of width below 6000 MeV. The upper edge of the range is chosen because an exotic state with higher mass would be expected to give a clearer signature in the $B^0 K^\pm$ final state [21]. The results are

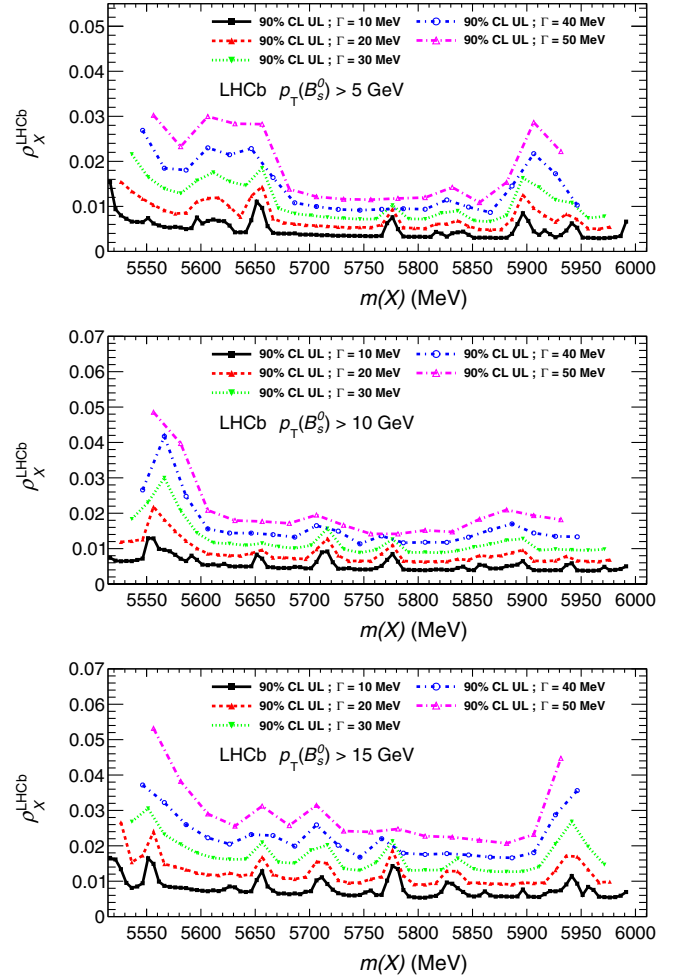


FIG. 3. Upper limits (ULs) at 90% confidence level (C.L.) as functions of the mass and width of a purported exotic state X decaying to $B_s^0 \pi^\pm$ with minimum $p_T(B_s^0)$ of (top) 5 GeV, (middle) 10 GeV, and (bottom) 15 GeV. The same limits also apply to a possible exotic meson decaying through the chain $B_s^{*0} \pi^\pm$, $B_s^{*0} \rightarrow B_s^0 \gamma$ where the photon is excluded from the reconstructed decays. In the latter case the nominal mass difference $m(B_s^{*0}) - m(B_s^0) = 48.6_{-1.6}^{+1.8}$ MeV [14] has to be added to the values on the x axis to get the mass of the exotic meson under investigation.

obtained in the same way as described above, and converted into upper limits that are shown in Fig. 3. The upper limits are weaker when a broader width is assumed, due to the larger amount of background under the putative peak. The limits also become weaker when there is an excess of events in the signal region, although all such excesses are consistent with being statistical fluctuations. The method used to set the upper limits smooths out any negative fluctuations.

In summary, a search for the claimed $X(5568)$ state has been carried out using a data sample corresponding to 3 fb^{-1} of pp collision data at $\sqrt{s} = 7$ and 8 TeV recorded by LHCb. No significant excess is found and thus the existence of the $X(5568)$ state is not confirmed. Upper limits are set on the relative production rate of the claimed state in the LHCb

acceptance. Limits are also set as a function of the mass and width of a possible exotic meson decaying to the $B_s^0\pi^\pm$ final state. The same limits also apply to a possible exotic meson decaying through the chain $B_s^{*0}\pi^\pm$, $B_s^{*0} \rightarrow B_s^0\gamma$ where the photon is excluded from the reconstructed decays.

We express our gratitude to our colleagues in the CERN accelerator departments for the excellent performance of the LHC. We thank the technical and administrative staff at the LHCb institutes. We acknowledge support from CERN and from the national agencies: CAPES, CNPq, FAPERJ and FINEP (Brazil); NSFC (China); CNRS/IN2P3 (France); BMBF, DFG and MPG (Germany); INFN (Italy); FOM and NWO (The Netherlands); MNiSW and NCN (Poland); MEN/IFA (Romania); MinES and FASO (Russia); MinECo (Spain); SNSF and SER (Switzerland); NASU (Ukraine); STFC (United Kingdom); NSF (USA). We acknowledge the computing resources that are provided by CERN, IN2P3 (France), KIT and DESY (Germany), INFN (Italy), SURF (The Netherlands), PIC (Spain), GridPP (United Kingdom), RRCKI and Yandex LLC (Russia), CSCS (Switzerland), IFIN-HH (Romania), CBPF (Brazil), PL-GRID (Poland) and OSC (USA). We are indebted to the communities behind the multiple open source software packages on which we depend. Individual groups or members have received support from AvH Foundation (Germany), EPLANET, Marie Skłodowska-Curie Actions and ERC (European Union), Conseil Général de Haute-Savoie, Labex ENIGMASS and OCEVU, Région Auvergne (France), RFBR and Yandex LLC (Russia), GVA, XuntaGal and GENCAT (Spain), Herchel Smith Fund, The Royal Society, Royal Commission for the Exhibition of 1851 and the Leverhulme Trust (United Kingdom).

[1] S. L. Olsen, A new hadron spectroscopy, *Front. Phys.* **10**, 121 (2015).
 [2] H.-Y. Cheng, Multiquark hadrons, *The Universe* **3**, 33 (2015).
 [3] V. M. Abazov *et al.* (D0 Collaboration), Evidence for a $B_s^0\pi^\pm$ State, *Phys. Rev. Lett.* **117**, 022003 (2016).
 [4] R. Aaij *et al.* (LHCb Collaboration), First Observation of the Decay $B_{s2}^*(5840)^0 \rightarrow B^{*+}K^-$ and Studies of Excited B_s^0 Mesons, *Phys. Rev. Lett.* **110**, 151803 (2013).
 [5] R. Aaij *et al.* (LHCb Collaboration), Precise measurements of the properties of the $B_1(5721)^{0,+}$ and $B_2^*(5747)^{0,+}$ states and observation of structure at higher invariant mass in

the $B^+\pi^-$ and $B^0\pi^+$ spectra, *J. High Energy Phys.* **04** (2015) 024.
 [6] A. A. Alves Jr. *et al.* (LHCb Collaboration), The LHCb detector at the LHC, *J. Instrum.* **3**, S08005 (2008).
 [7] R. Aaij *et al.* (LHCb Collaboration), LHCb detector performance, *Int. J. Mod. Phys. A* **30**, 1530022 (2015).
 [8] T. Sjöstrand, S. Mrenna, and P. Skands, PYTHIA 6.4 physics and manual, *J. High Energy Phys.* **05** (2006) 026; T. Sjöstrand, S. Mrenna, and P. Skands, A brief introduction to PYTHIA 8.1, *Comput. Phys. Commun.* **178**, 852 (2008).
 [9] I. Belyaev *et al.*, Handling of the generation of primary events in Gauss, the LHCb simulation framework, *J. Phys. Conf. Ser.* **331**, 032047 (2011).
 [10] D. J. Lange, The EvtGen particle decay simulation package, *Nucl. Instrum. Methods Phys. Res., Sect. A* **462**, 152 (2001).
 [11] P. Golonka and Z. Was, PHOTOS Monte Carlo: A precision tool for QED corrections in Z and W decays, *Eur. Phys. J. C* **45**, 97 (2006).
 [12] J. Allison *et al.* (Geant4 Collaboration), Geant4 developments and applications, *IEEE Trans. Nucl. Sci.* **53**, 270 (2006); S. Agostinelli *et al.* (Geant4 Collaboration), Geant4: A simulation toolkit, *Nucl. Instrum. Methods Phys. Res., Sect. A* **506**, 250 (2003).
 [13] M. Clemencic, G. Corti, S. Easo, C. R. Jones, S. Miglioranz, M. Pappagallo, and P. Robbe, The LHCb simulation application, Gauss: Design, evolution and experience, *J. Phys. Conf. Ser.* **331**, 032023 (2011).
 [14] K. A. Olive *et al.* (Particle Data Group Collaboration), Review of particle physics, *Chin. Phys. C* **38**, 090001 (2014), and 2015 update.
 [15] R. Aaij *et al.* (LHCb Collaboration), Amplitude analysis and branching fraction measurement of $\bar{B}_s^0 \rightarrow J/\psi K^+ K^-$, *Phys. Rev. D* **87**, 072004 (2013).
 [16] W. D. Hulsbergen, Decay chain fitting with a Kalman filter, *Nucl. Instrum. Methods Phys. Res., Sect. A* **552**, 566 (2005).
 [17] R. Aaij *et al.* (LHCb Collaboration), Measurement of B meson production cross-sections in proton-proton collisions at $\sqrt{s} = 7$ TeV, *J. High Energy Phys.* **08** (2013) 117.
 [18] M. Adinolfi *et al.*, Performance of the LHCb RICH detector at the LHC, *Eur. Phys. J. C* **73**, 2431 (2013).
 [19] R. Aaij *et al.* (LHCb Collaboration), Measurement of the track reconstruction efficiency at LHCb, *J. Instrum.* **10**, P02007 (2015).
 [20] R. Aaij *et al.* (LHCb Collaboration), Observation of the Decay $B_c^+ \rightarrow B_s^0\pi^+$, *Phys. Rev. Lett.* **111**, 181801 (2013).
 [21] A. Esposito, A. Pilloni, and A. D. Polosa, Hybridized tetraquarks, *Phys. Lett. B* **758**, 292 (2016).

R. Aaij,⁴⁰ B. Adeva,³⁹ M. Adinolfi,⁴⁸ Z. Ajaltouni,⁵ S. Akar,⁶ J. Albrecht,¹⁰ F. Alessio,⁴⁰ M. Alexander,⁵³ S. Ali,⁴³ G. Alkhazov,³¹ P. Alvarez Cartelle,⁵⁵ A. A. Alves Jr.,⁵⁹ S. Amato,² S. Amerio,²³ Y. Amhis,⁷ L. An,⁴¹ L. Anderlini,¹⁸ G. Andreassi,⁴¹ M. Andreotti,^{17,a} J. E. Andrews,⁶⁰ R. B. Appleby,⁵⁶ F. Archilli,⁴³ P. d'Argent,¹² J. Arnau Romeu,⁶ A. Artamonov,³⁷ M. Artuso,⁶¹ E. Aslanides,⁶ G. Auriemma,²⁶ M. Baalouch,⁵ I. Babuschkin,⁵⁶ S. Bachmann,¹² J. J. Back,⁵⁰

A. Badalov,³⁸ C. Baesso,⁶² S. Baker,⁵⁵ W. Baldini,¹⁷ R. J. Barlow,⁵⁶ C. Barschel,⁴⁰ S. Barsuk,⁷ W. Barter,⁴⁰ M. Baszczyk,²⁷ V. Batozskaya,²⁹ B. Batsukh,⁶¹ V. Battista,⁴¹ A. Bay,⁴¹ L. Beaucourt,⁴ J. Beddow,⁵³ F. Bedeschi,²⁴ I. Bediaga,¹ L. J. Bel,⁴³ V. Bellee,⁴¹ N. Belloli,^{21,b} K. Belous,³⁷ I. Belyaev,³² E. Ben-Haim,⁸ G. Bencivenni,¹⁹ S. Benson,⁴³ J. Benton,⁴⁸ A. Berezhnoy,³³ R. Bernet,⁴² A. Bertolin,²³ F. Betti,¹⁵ M.-O. Bettler,⁴⁰ M. van Beuzekom,⁴³ I. A. Bezshyiko,⁴² S. Bifani,⁴⁷ P. Billoir,⁸ T. Bird,⁵⁶ A. Birnkraut,¹⁰ A. Bitadze,⁵⁶ A. Bizzeti,^{18,c} T. Blake,⁵⁰ F. Blanc,⁴¹ J. Blouw,¹¹ S. Blusk,⁶¹ V. Bocci,²⁶ T. Boettcher,⁵⁸ A. Bondar,^{36,d} N. Bondar,^{31,40} W. Bonivento,¹⁶ A. Borgheresi,^{21,b} S. Borghi,⁵⁶ M. Borisyak,³⁵ M. Borsato,³⁹ F. Bossu,⁷ M. Boudir,⁹ T. J. V. Bowcock,⁵⁴ E. Bowen,⁴² C. Bozzi,^{17,40} S. Braun,¹² M. Britsch,¹² T. Britton,⁶¹ J. Brodzicka,⁵⁶ E. Buchanan,⁴⁸ C. Burr,⁵⁶ A. Bursche,² J. Buytaert,⁴⁰ S. Cadgeddu,¹⁶ R. Calabrese,^{17,a} M. Calvi,^{21,b} M. Calvo Gomez,^{38,e} A. Camboni,³⁸ P. Campana,¹⁹ D. Campora Perez,⁴⁰ D. H. Campora Perez,⁴⁰ L. Capriotti,⁵⁶ A. Carbone,^{15,f} G. Carboni,^{25,g} R. Cardinale,^{20,h} A. Cardini,¹⁶ P. Carniti,^{21,b} L. Carson,⁵² K. Carvalho Akiba,² G. Casse,⁵⁴ L. Cassina,^{21,b} L. Castillo Garcia,⁴¹ M. Cattaneo,⁴⁰ Ch. Cauet,¹⁰ G. Cavallero,²⁰ R. Cenci,^{24,i} M. Charles,⁸ Ph. Charpentier,⁴⁰ G. Chatzikonstantinidis,⁴⁷ M. Chefdeville,⁴ S. Chen,⁵⁶ S.-F. Cheung,⁵⁷ V. Chobanova,³⁹ M. Chruszcz,^{42,27} X. Cid Vidal,³⁹ G. Ciezarek,⁴³ P. E. L. Clarke,⁵² M. Clemencic,⁴⁰ H. V. Cliff,⁴⁹ J. Closier,⁴⁰ V. Coco,⁵⁹ J. Cogan,⁶ E. Cogneras,⁵ V. Cogoni,^{16,40,j} L. Cojocariu,³⁰ P. Collins,⁴⁰ A. Comerma-Montells,¹² A. Contu,⁴⁰ A. Cook,⁴⁸ S. Coquereau,³⁸ G. Corti,⁴⁰ M. Corvo,^{17,a} C. M. Costa Sobral,⁵⁰ B. Couturier,⁴⁰ G. A. Cowan,⁵² D. C. Craik,⁵² A. Crocombe,⁵⁰ M. Cruz Torres,⁶² S. Cunliffe,⁵⁵ R. Currie,⁵⁵ C. D'Ambrosio,⁴⁰ F. Da Cunha Marinho,² E. Dall'Occo,⁴³ J. Dalseno,⁴⁸ P. N. Y. David,⁴³ A. Davis,⁵⁹ O. De Aguiar Francisco,² K. De Bruyn,⁶ S. De Capua,⁵⁶ M. De Cian,¹² J. M. De Miranda,¹ L. De Paula,² M. De Serio,^{14,k} P. De Simone,¹⁹ C. T. Dean,⁵³ D. Decamp,⁴ M. Deckenhoff,¹⁰ L. Del Buono,⁸ M. Demmer,¹⁰ D. Derkach,³⁵ O. Deschamps,⁵ F. Dettori,⁴⁰ B. Dey,²² A. Di Canto,⁴⁰ H. Dijkstra,⁴⁰ F. Dordei,⁴⁰ M. Dorigo,⁴¹ A. Dosil Suárez,³⁹ A. Dovbnya,⁴⁵ K. Dreimanis,⁵⁴ L. Dufour,⁴³ G. Dujany,⁵⁶ K. Dungs,⁴⁰ P. Durante,⁴⁰ R. Dzhelyadin,³⁷ A. Dziurda,⁴⁰ A. Dzyuba,³¹ N. Déleage,⁴ S. Easo,⁵¹ M. Ebert,⁵² U. Egede,⁵⁵ V. Egorychev,³² S. Eidelman,^{36,d} S. Eisenhardt,⁵² U. Eitschberger,¹⁰ R. Ekelhof,¹⁰ L. Eklund,⁵³ Ch. Elsasser,⁴² S. Ely,⁶¹ S. Esen,¹² H. M. Evans,⁴⁹ T. Evans,⁵⁷ A. Falabella,¹⁵ N. Farley,⁴⁷ S. Farry,⁵⁴ R. Fay,⁵⁴ D. Fazzini,^{21,b} D. Ferguson,⁵² V. Fernandez Albor,³⁹ A. Fernandez Prieto,³⁹ F. Ferrari,^{15,40} F. Ferreira Rodrigues,¹ M. Ferro-Luzzi,⁴⁰ S. Filippov,³⁴ R. A. Fini,¹⁴ M. Fiore,^{17,a} M. Fiorini,^{17,a} M. Firlej,²⁸ C. Fitzpatrick,⁴¹ T. Fiutowski,²⁸ F. Fleuret,⁷¹ K. Fohl,⁴⁰ M. Fontana,^{16,40} F. Fontanelli,^{20,h} D. C. Forshaw,⁶¹ R. Forty,⁴⁰ V. Franco Lima,⁵⁴ M. Frank,⁴⁰ C. Frei,⁴⁰ J. Fu,^{22,m} E. Furfaro,^{25,g} C. Färber,⁴⁰ A. Gallas Torreira,³⁹ D. Galli,^{15,f} S. Gallorini,²³ S. Gambetta,⁵² M. Gandelman,² P. Gandini,⁵⁷ Y. Gao,³ L. M. Garcia Martin,⁶⁸ J. García Pardiñas,³⁹ J. Garra Tico,⁴⁹ L. Garrido,³⁸ P. J. Garsed,⁴⁹ D. Gascon,³⁸ C. Gaspar,⁴⁰ L. Gavardi,¹⁰ G. Gazzoni,⁵ D. Gerick,¹² E. Gersabeck,¹² M. Gersabeck,⁵⁶ T. Gershon,⁵⁰ Ph. Ghez,⁴ S. Gianì,⁴¹ V. Gibson,⁴⁹ O. G. Girard,⁴¹ L. Giubega,³⁰ K. Gizdov,⁵² V. V. Gligorov,⁸ D. Golubkov,³² A. Golutvin,^{55,40} A. Gomes,^{1,n} I. V. Gorelov,³³ C. Gotti,^{21,b} M. Grabalosa Gándara,⁵ R. Graciani Diaz,³⁸ L. A. Granado Cardoso,⁴⁰ E. Graugés,³⁸ E. Graverini,⁴² G. Graziani,¹⁸ A. Grecu,³⁰ P. Griffith,⁴⁷ L. Grillo,^{21,40,b} B. R. Gruber Cazon,⁵⁷ O. Grünberg,⁶⁶ E. Gushchin,³⁴ Yu. Guz,³⁷ T. Gys,⁴⁰ C. Göbel,⁶² T. Hadavizadeh,⁵⁷ C. Hadjivasiliou,⁵ G. Haefeli,⁴¹ C. Haen,⁴⁰ S. C. Haines,⁴⁹ S. Hall,⁵⁵ B. Hamilton,⁶⁰ X. Han,¹² S. Hansmann-Menzemer,¹² N. Harnew,⁵⁷ S. T. Harnew,⁴⁸ J. Harrison,⁵⁶ M. Hatch,⁴⁰ J. He,⁶³ T. Head,⁴¹ A. Heister,⁹ K. Hennessy,⁵⁴ P. Henrard,⁵ L. Henry,⁸ J. A. Hernando Morata,³⁹ E. van Herwijnen,⁴⁰ M. Heß,⁶⁶ A. Hicheur,² D. Hill,⁵⁷ C. Hombach,⁵⁶ H. Hopchev,⁴¹ W. Hulsbergen,⁴³ T. Humair,⁵⁵ M. Hushchyn,³⁵ N. Hussain,⁵⁷ D. Hutchcroft,⁵⁴ M. Idzik,²⁸ P. Ilten,⁵⁸ R. Jacobsson,⁴⁰ A. Jaeger,¹² J. Jalocha,⁵⁷ E. Jans,⁴³ A. Jawahery,⁶⁰ F. Jiang,³ M. John,⁵⁷ D. Johnson,⁴⁰ C. R. Jones,⁴⁹ C. Joram,⁴⁰ B. Jost,⁴⁰ N. Jurik,⁶¹ S. Kandybei,⁴⁵ W. Kalso,⁶ M. Karacson,⁴⁰ J. M. Kariuki,⁴⁸ S. Karodia,⁵³ M. Kecke,¹² M. Kelsey,⁶¹ I. R. Kenyon,⁴⁷ M. Kenzie,⁴⁹ T. Ketel,⁴⁴ E. Khairullin,³⁵ B. Khanji,^{21,40,b} C. Khurewathanakul,⁴¹ T. Kirn,⁹ S. Klaver,⁵⁶ K. Klimaszewski,²⁹ S. Koliev,⁴⁶ M. Kolpin,¹² I. Komarov,⁴¹ R. F. Koopman,⁴⁴ P. Koppenburg,⁴³ A. Kozachuk,³³ M. Kozeiha,⁵ L. Kravchuk,³⁴ K. Kreplin,¹² M. Krepis,⁵⁰ P. Krokovny,^{36,d} F. Kruse,¹⁰ W. Krzemien,²⁹ W. Kucewicz,^{27,o} M. Kucharczyk,²⁷ V. Kudryavtsev,^{36,d} A. K. Kuonen,⁴¹ K. Kurek,²⁹ T. Kvaratskheliya,^{32,40} D. Lacarrere,⁴⁰ G. Lafferty,⁵⁶ A. Lai,¹⁶ D. Lambert,⁵² G. Lanfranchi,¹⁹ C. Langenbruch,⁹ T. Latham,⁵⁰ C. Lazzeroni,⁴⁷ R. Le Gac,⁶ J. van Leerdam,⁴³ J.-P. Lees,⁴ A. Leflat,^{33,40} J. Lefrançois,⁷ R. Lefèvre,⁵ F. Lemaître,⁴⁰ E. Lemos Cid,³⁹ O. Leroy,⁶ T. Lesiak,²⁷ B. Leverington,¹² Y. Li,⁷ T. Likhomanenko,^{35,67} R. Lindner,⁴⁰ C. Linn,⁴⁰ F. Lionetto,⁴² B. Liu,¹⁶ X. Liu,³ D. Loh,⁵⁰ I. Longstaff,⁵³ J. H. Lopes,² D. Lucchesi,^{23,p} M. Lucio Martinez,³⁹ H. Luo,⁵² A. Lupato,²³ E. Luppi,^{17,a} O. Lupton,⁵⁷ A. Lusiani,²⁴ X. Lyu,⁶³ F. Machefert,⁷ F. Maciuc,³⁰ O. Maev,³¹ K. Maguire,⁵⁶ S. Malde,⁵⁷ A. Malinin,⁶⁷ T. Maltsev,³⁶ G. Manca,⁷ G. Mancinelli,⁶ P. Manning,⁶¹ J. Maratas,^{5,q} J. F. Marchand,⁴ U. Marconi,¹⁵ C. Marin Benito,³⁸ P. Marino,^{24,i} J. Marks,¹² G. Martellotti,²⁶ M. Martin,⁶ M. Martinelli,⁴¹ D. Martinez Santos,³⁹ F. Martinez Vidal,⁶⁸ D. Martins Tostes,²

L. M. Massacrier,⁷ A. Massafferri,¹ R. Matev,⁴⁰ A. Mathad,⁵⁰ Z. Mathe,⁴⁰ C. Matteuzzi,²¹ A. Mauri,⁴² B. Maurin,⁴¹ A. Mazurov,⁴⁷ M. McCann,⁵⁵ J. McCarthy,⁴⁷ A. McNab,⁵⁶ R. McNulty,¹³ B. Meadows,⁵⁹ F. Meier,¹⁰ M. Meissner,¹² D. Melnychuk,²⁹ M. Merk,⁴³ A. Merli,^{22,m} E. Michielin,²³ D. A. Milanes,⁶⁵ M.-N. Minard,⁴ D. S. Mitzel,¹² A. Mogini,⁸ J. Molina Rodriguez,⁶² I. A. Monroy,⁶⁵ S. Monteil,⁵ M. Morandin,²³ P. Morawski,²⁸ A. Mordà,⁶ M. J. Morello,^{24,i} J. Moron,²⁸ A. B. Morris,⁵² R. Mountain,⁶¹ F. Muheim,⁵² M. Mulder,⁴³ M. Mussini,¹⁵ D. Müller,⁵⁶ J. Müller,¹⁰ K. Müller,⁴² V. Müller,¹⁰ P. Naik,⁴⁸ T. Nakada,⁴¹ R. Nandakumar,⁵¹ A. Nandi,⁵⁷ I. Nasteva,² M. Needham,⁵² N. Neri,²² S. Neubert,¹² N. Neufeld,⁴⁰ M. Neuner,¹² A. D. Nguyen,⁴¹ C. Nguyen-Mau,^{41,r} S. Nieswand,⁹ R. Niet,¹⁰ N. Nikitin,³³ T. Nikodem,¹² A. Novoselov,³⁷ D. P. O'Hanlon,⁵⁰ A. Oblakowska-Mucha,²⁸ V. Obraztsov,³⁷ S. Ogilvy,¹⁹ R. Oldeman,⁴⁹ C. J. G. Onderwater,⁶⁹ J. M. Otalora Goicochea,² A. Otto,⁴⁰ P. Owen,⁴² A. Oyanguren,⁶⁸ P. R. Pais,⁴¹ A. Palano,^{14,k} F. Palombo,^{22,m} M. Palutan,¹⁹ J. Panman,⁴⁰ A. Papanestis,⁵¹ M. Pappagallo,^{14,k} L. L. Pappalardo,^{17,a} W. Parker,⁶⁰ C. Parkes,⁵⁶ G. Passaleva,¹⁸ A. Pastore,^{14,k} G. D. Patel,⁵⁴ M. Patel,⁵⁵ C. Patrignani,^{15,f} A. Pearce,^{56,51} A. Pellegrino,⁴³ G. Penso,²⁶ M. Pepe Altarelli,⁴⁰ S. Perazzini,⁴⁰ P. Perret,⁵ L. Pescatore,⁴⁷ K. Petridis,⁴⁸ A. Petrolini,^{20,h} A. Petrov,⁶⁷ M. Petruzzo,^{22,m} E. Picatoste Olloqui,³⁸ B. Pietrzyk,⁴ M. Pikies,²⁷ D. Pinci,²⁶ A. Pistone,²⁰ A. Piucci,¹² S. Playfer,⁵² M. Plo Casasus,³⁹ T. Poikela,⁴⁰ F. Polci,⁸ A. Poluektov,^{50,36} I. Polyakov,⁶¹ E. Polycarpo,² G. J. Pomery,⁴⁸ A. Popov,³⁷ D. Popov,^{11,40} B. Popovici,³⁰ S. Poslavskii,³⁷ C. Potterat,² E. Price,⁴⁸ J. D. Price,⁵⁴ J. Prisciandaro,³⁹ A. Pritchard,⁵⁴ C. Prouve,⁴⁸ V. Pugatch,⁴⁶ A. Puig Navarro,⁴¹ G. Punzi,^{24,s} W. Qian,⁵⁷ R. Quagliani,^{7,48} B. Rachwal,²⁷ J. H. Rademacker,⁴⁸ M. Rama,²⁴ M. Ramos Pernas,³⁹ M. S. Rangel,² I. Raniuk,⁴⁵ G. Raven,⁴⁴ F. Redi,⁵⁵ S. Reichert,¹⁰ A. C. dos Reis,¹ C. Remon Alepuz,⁶⁸ V. Renaudin,⁷ S. Ricciardi,⁵¹ S. Richards,⁴⁸ M. Rihl,⁴⁰ K. Rinnert,⁵⁴ V. Rives Molina,³⁸ P. Robbe,^{7,40} A. B. Rodrigues,¹ E. Rodrigues,⁵⁹ J. A. Rodriguez Lopez,⁶⁵ P. Rodriguez Perez,⁵⁶ A. Rogozhnikov,³⁵ S. Roiser,⁴⁰ V. Romanovskiy,³⁷ A. Romero Vidal,³⁹ J. W. Ronayne,¹³ M. Rotondo,¹⁹ M. S. Rudolph,⁶¹ T. Ruf,⁴⁰ P. Ruiz Valls,⁶⁸ J. J. Saborido Silva,³⁹ E. Sadykhov,³² N. Sagidova,³¹ B. Saitta,^{16,j} V. Salustino Guimaraes,² C. Sanchez Mayordomo,⁶⁸ B. Sanmartin Sedes,³⁹ R. Santacesaria,²⁶ C. Santamarina Rios,³⁹ M. Santimaria,¹⁹ E. Santovetti,^{25,g} A. Sarti,^{19,t} C. Satriano,^{26,u} A. Satta,²⁵ D. M. Saunders,⁴⁸ D. Savrina,^{32,33} S. Schael,⁹ M. Schellenberg,¹⁰ M. Schiller,⁴⁰ H. Schindler,⁴⁰ M. Schlupp,¹⁰ M. Schmelling,¹¹ T. Schmelzer,¹⁰ B. Schmidt,⁴⁰ O. Schneider,⁴¹ A. Schopper,⁴⁰ K. Schubert,¹⁰ M. Schubiger,⁴¹ M.-H. Schune,⁷ R. Schwemmer,⁴⁰ B. Sciascia,¹⁹ A. Sciubba,^{26,t} A. Semennikov,³² A. Sergi,⁴⁷ N. Serra,⁴² J. Serrano,⁶ L. Sestini,²³ P. Seyfert,²¹ M. Shapkin,³⁷ I. Shapoval,⁴⁵ Y. Shcheglov,³¹ T. Shears,⁵⁴ L. Shekhtman,^{36,d} V. Shevchenko,⁶⁷ A. Shires,¹⁰ B. G. Siddi,^{17,40} R. Silva Coutinho,⁴² L. Silva de Oliveira,² G. Simi,^{23,p} S. Simone,^{14,k} M. Sirendi,⁴⁹ N. Skidmore,⁴⁸ T. Skwarnicki,⁶¹ E. Smith,⁵⁵ I. T. Smith,⁵² J. Smith,⁴⁹ M. Smith,⁵⁵ H. Snoek,⁴³ M. D. Sokoloff,⁵⁹ F. J. P. Soler,⁵³ B. Souza De Paula,² B. Spaan,¹⁰ P. Spradlin,⁵³ S. Sridharan,⁴⁰ F. Stagni,⁴⁰ M. Stahl,¹² S. Stahl,⁴⁰ P. Stefko,⁴¹ S. Stefkova,⁵⁵ O. Steinkamp,⁴² S. Stemmle,¹² O. Stenyakin,³⁷ S. Stevenson,⁵⁷ S. Stoica,³⁰ S. Stone,⁶¹ B. Storaci,⁴² S. Stracka,^{24,s} M. Straticiu,³⁰ U. Straumann,⁴² L. Sun,⁵⁹ W. Sutcliffe,⁵⁵ K. Swientek,²⁸ V. Syropoulos,⁴⁴ M. Szczekowski,²⁹ T. Szumlak,²⁸ S. T'Jampens,⁴ A. Tayduganov,⁶ T. Tekampe,¹⁰ M. Teklishyn,⁷ G. Tellarini,^{17,a} F. Teubert,⁴⁰ E. Thomas,⁴⁰ J. van Tilburg,⁴³ M. J. Tilley,⁵⁵ V. Tisserand,⁴ M. Tobin,⁴¹ S. Tolk,⁴⁹ L. Tomassetti,^{17,a} D. Tonelli,⁴⁰ S. Topp-Joergensen,⁵⁷ F. Toriello,⁶¹ E. Tournefier,⁴ S. Tourneur,⁴¹ K. Trabelsi,⁴¹ M. Traill,⁵³ M. T. Tran,⁴¹ M. Tresch,⁴² A. Trisovic,⁴⁰ A. Tsaregorodtsev,⁶ P. Tsopelas,⁴³ A. Tully,⁴⁹ N. Tuning,⁴³ A. Ukleja,²⁹ A. Ustyuzhanin,^{35,67} U. Uwer,¹² C. Vacca,^{16,j} V. Vagnoni,^{15,40} A. Valassi,⁴⁰ S. Valat,⁴⁰ G. Valenti,¹⁵ A. Vallier,⁷ R. Vazquez Gomez,¹⁹ P. Vazquez Regueiro,³⁹ S. Vecchi,¹⁷ M. van Veghel,⁴³ J. J. Velthuis,⁴⁸ M. Veltri,^{18,v} G. Veneziano,⁴¹ A. Venkateswaran,⁶¹ M. Vernet,⁵ M. Vesterinen,¹² B. Viaud,⁷ D. Vieira,¹ M. Vieites Diaz,³⁹ X. Vilasis-Cardona,^{38,e} V. Volkov,³³ A. Vollhardt,⁴² B. Voneki,⁴⁰ A. Vorobyev,³¹ V. Vorobyev,^{36,d} C. Voß,⁶⁶ J. A. de Vries,⁴³ C. Vázquez Sierra,³⁹ R. Waldi,⁶⁶ C. Wallace,⁵⁰ R. Wallace,¹³ J. Walsh,²⁴ J. Wang,⁶¹ D. R. Ward,⁴⁹ H. M. Wark,⁵⁴ N. K. Watson,⁴⁷ D. Websdale,⁵⁵ A. Weiden,⁴² M. Whitehead,⁴⁰ J. Wicht,⁵⁰ G. Wilkinson,^{57,40} M. Wilkinson,⁶¹ M. Williams,⁴⁰ M. P. Williams,⁴⁷ M. Williams,⁵⁸ T. Williams,⁴⁷ F. F. Wilson,⁵¹ J. Wimberley,⁶⁰ J. Wishahi,¹⁰ W. Wislicki,²⁹ M. Witek,²⁷ G. Wormser,⁷ S. A. Wotton,⁴⁹ K. Wraight,⁵³ S. Wright,⁴⁹ K. Wyllie,⁴⁰ Y. Xie,⁶⁴ Z. Xing,⁶¹ Z. Xu,⁴¹ Z. Yang,³ H. Yin,⁶⁴ J. Yu,⁶⁴ X. Yuan,^{36,d} O. Yushchenko,³⁷ K. A. Zarebski,⁴⁷ M. Zavertyaev,^{11,w} L. Zhang,³ Y. Zhang,⁷ A. Zhelezov,¹² Y. Zheng,⁶³ A. Zhokhov,³² X. Zhu,³ V. Zhukov,⁹ and S. Zucchelli¹⁵

(LHCb Collaboration)

- ¹Centro Brasileiro de Pesquisas Físicas (CBPF), Rio de Janeiro, Brazil
²Universidade Federal do Rio de Janeiro (UFRJ), Rio de Janeiro, Brazil
³Center for High Energy Physics, Tsinghua University, Beijing, China
⁴LAPP, Université Savoie Mont-Blanc, CNRS/IN2P3, Annecy-Le-Vieux, France
⁵Clermont Université, Université Blaise Pascal, CNRS/IN2P3, LPC, Clermont-Ferrand, France
⁶CPPM, Aix-Marseille Université, CNRS/IN2P3, Marseille, France
⁷LAL, Université Paris-Sud, CNRS/IN2P3, Orsay, France
⁸LPNHE, Université Pierre et Marie Curie, Université Paris Diderot, CNRS/IN2P3, Paris, France
⁹I. Physikalisches Institut, RWTH Aachen University, Aachen, Germany
¹⁰Fakultät Physik, Technische Universität Dortmund, Dortmund, Germany
¹¹Max-Planck-Institut für Kernphysik (MPIK), Heidelberg, Germany
¹²Physikalisches Institut, Ruprecht-Karls-Universität Heidelberg, Heidelberg, Germany
¹³School of Physics, University College Dublin, Dublin, Ireland
¹⁴Sezione INFN di Bari, Bari, Italy
¹⁵Sezione INFN di Bologna, Bologna, Italy
¹⁶Sezione INFN di Cagliari, Cagliari, Italy
¹⁷Sezione INFN di Ferrara, Ferrara, Italy
¹⁸Sezione INFN di Firenze, Firenze, Italy
¹⁹Laboratori Nazionali dell'INFN di Frascati, Frascati, Italy
²⁰Sezione INFN di Genova, Genova, Italy
²¹Sezione INFN di Milano Bicocca, Milano, Italy
²²Sezione INFN di Milano, Milano, Italy
²³Sezione INFN di Padova, Padova, Italy
²⁴Sezione INFN di Pisa, Pisa, Italy
²⁵Sezione INFN di Roma Tor Vergata, Roma, Italy
²⁶Sezione INFN di Roma La Sapienza, Roma, Italy
²⁷Henryk Niewodniczanski Institute of Nuclear Physics Polish Academy of Sciences, Kraków, Poland
²⁸AGH - University of Science and Technology, Faculty of Physics and Applied Computer Science, Kraków, Poland
²⁹National Center for Nuclear Research (NCBJ), Warsaw, Poland
³⁰Horia Hulubei National Institute of Physics and Nuclear Engineering, Bucharest-Magurele, Romania
³¹Petersburg Nuclear Physics Institute (PNPI), Gatchina, Russia
³²Institute of Theoretical and Experimental Physics (ITEP), Moscow, Russia
³³Institute of Nuclear Physics, Moscow State University (SINP MSU), Moscow, Russia
³⁴Institute for Nuclear Research of the Russian Academy of Sciences (INR RAN), Moscow, Russia
³⁵Yandex School of Data Analysis, Moscow, Russia
³⁶Budker Institute of Nuclear Physics (SB RAS), Novosibirsk, Russia
³⁷Institute for High Energy Physics (IHEP), Protvino, Russia
³⁸ICCUB, Universitat de Barcelona, Barcelona, Spain
³⁹Universidad de Santiago de Compostela, Santiago de Compostela, Spain
⁴⁰European Organization for Nuclear Research (CERN), Geneva, Switzerland
⁴¹Institute of Physics, Ecole Polytechnique Fédérale de Lausanne (EPFL), Lausanne, Switzerland
⁴²Physik-Institut, Universität Zürich, Zürich, Switzerland
⁴³Nikhef National Institute for Subatomic Physics, Amsterdam, Netherlands
⁴⁴Nikhef National Institute for Subatomic Physics and VU University Amsterdam, Amsterdam, Netherlands
⁴⁵NSC Kharkiv Institute of Physics and Technology (NSC KIPT), Kharkiv, Ukraine
⁴⁶Institute for Nuclear Research of the National Academy of Sciences (KINR), Kyiv, Ukraine
⁴⁷University of Birmingham, Birmingham, United Kingdom
⁴⁸H.H. Wills Physics Laboratory, University of Bristol, Bristol, United Kingdom
⁴⁹Cavendish Laboratory, University of Cambridge, Cambridge, United Kingdom
⁵⁰Department of Physics, University of Warwick, Coventry, United Kingdom
⁵¹STFC Rutherford Appleton Laboratory, Didcot, United Kingdom
⁵²School of Physics and Astronomy, University of Edinburgh, Edinburgh, United Kingdom
⁵³School of Physics and Astronomy, University of Glasgow, Glasgow, United Kingdom
⁵⁴Oliver Lodge Laboratory, University of Liverpool, Liverpool, United Kingdom
⁵⁵Imperial College London, London, United Kingdom
⁵⁶School of Physics and Astronomy, University of Manchester, Manchester, United Kingdom
⁵⁷Department of Physics, University of Oxford, Oxford, United Kingdom
⁵⁸Massachusetts Institute of Technology, Cambridge, Massachusetts, USA
⁵⁹University of Cincinnati, Cincinnati, Ohio, USA
⁶⁰University of Maryland, College Park, Maryland, USA

⁶¹*Syracuse University, Syracuse, New York, USA*

⁶²*Pontificia Universidade Católica do Rio de Janeiro (PUC-Rio), Rio de Janeiro, Brazil
(associated with Universidade Federal do Rio de Janeiro (UFRJ), Rio de Janeiro, Brazil)*

⁶³*University of Chinese Academy of Sciences, Beijing, China
(associated with Center for High Energy Physics, Tsinghua University, Beijing, China)*

⁶⁴*Institute of Particle Physics, Central China Normal University, Wuhan, Hubei, China
(associated with Center for High Energy Physics, Tsinghua University, Beijing, China)*

⁶⁵*Departamento de Física, Universidad Nacional de Colombia, Bogota, Colombia
(associated with LPNHE, Université Pierre et Marie Curie, Université Paris Diderot, CNRS/IN2P3, Paris, France)*

⁶⁶*Institut für Physik, Universität Rostock, Rostock, Germany
(associated with Physikalisches Institut, Ruprecht-Karls-Universität Heidelberg, Heidelberg, Germany)*

⁶⁷*National Research Centre Kurchatov Institute, Moscow, Russia
(associated with Institute of Theoretical and Experimental Physics (ITEP), Moscow, Russia)*

⁶⁸*Instituto de Física Corpuscular, Centro Mixto Universidad de Valencia - CSIC, Valencia, Spain
(associated with ICCUB, Universitat de Barcelona, Barcelona, Spain)*

⁶⁹*Van Swinderen Institute, University of Groningen, Groningen, Netherlands
(associated with Nikhef National Institute for Subatomic Physics, Amsterdam, Netherlands)*

^aAlso at Università di Ferrara, Ferrara, Italy.

^bAlso at Università di Milano Bicocca, Milano, Italy.

^cAlso at Università di Modena e Reggio Emilia, Modena, Italy.

^dAlso at Novosibirsk State University, Novosibirsk, Russia.

^eAlso at LIFAELS, La Salle, Universitat Ramon Llull, Barcelona, Spain.

^fAlso at Università di Bologna, Bologna, Italy.

^gAlso at Università di Roma Tor Vergata, Roma, Italy.

^hAlso at Università di Genova, Genova, Italy.

ⁱAlso at Scuola Normale Superiore, Pisa, Italy.

^jAlso at Università di Cagliari, Cagliari, Italy.

^kAlso at Università di Bari, Bari, Italy.

^lAlso at Laboratoire Leprince-Ringuet, Palaiseau, France.

^mAlso at Università degli Studi di Milano, Milano, Italy.

ⁿAlso at Universidade Federal do Triângulo Mineiro (UFTM), Uberaba-MG, Brazil.

^oAlso at AGH - University of Science and Technology, Faculty of Computer Science, Electronics and Telecommunications, Kraków, Poland.

^pAlso at Università di Padova, Padova, Italy.

^qAlso at Iligan Institute of Technology (IIT), Iligan, Philippines.

^rAlso at Hanoi University of Science, Hanoi, Viet Nam.

^sAlso at Università di Pisa, Pisa, Italy.

^tAlso at Università di Roma La Sapienza, Roma, Italy.

^uAlso at Università della Basilicata, Potenza, Italy.

^vAlso at Università di Urbino, Urbino, Italy.

^wAlso at P.N. Lebedev Physical Institute, Russian Academy of Science (LPI RAS), Moscow, Russia.